Available online at www.sciencedirect.com
ScienceDirect
Journal of Power Sources 173 (2007) 748–754
JOURNAL OF POWER SOURCES
www.elsevier.com/locate/jpowsour

Mesoscale models of ac conductivity in composite polymeric electrolytes

M. Siekierski *, K. Nadara

Faculty of Chemistry, Warsaw University of Technology, Noakowskiego 3, 00-664 Warsaw, Poland

Available online 21 May 2007

Abstract

The presented paper shows a possibility of creation of a useful and efficient model of conductivity for composite polymeric electrolytes. It deals with a more elaborate and versatile mesoscale approach (in comparison to the already applied Effective Medium Theory approach for which each new composite microstructure forces a new mixing rule development) based on the Random Resistor Network method. The introduced model can predict the ac conductivity values for a whole spectrum of frequencies for different composites with a wide range of possible microstructures. It is based on complex current iteration procedure for a randomly generated three-dimensional network of impedances constituting a digital image of the electric properties of the virtual sample studied. A spatial unit of the material present in the sample is defined as a parallel *RC* connection.

Keywords: Mesoscale; Composite polymeric electrolytes; Effective Medium Theory; Random Resistor Network

1. Introduction

Semicrystalline polymeric electrolytes based on poly(ethylene oxide) matrix reveal good mechanical and electrochemical properties unfortunately together with low electrical conductivity being the main limitation of their application. An improvement of electrical conductivity with a parallel further increase of the stability can be achieved by the formation of composite materials. They are produced through the addition of an electrically insulating filler (ceramic powders, immiscible polymers) to the pristine solid electrolyte. The obtained materials can be applied to various electrochemical systems such as lithium–polymer batteries [1]. The micromorphology of the sample can be described as a suspension of the randomly distributed filler grains in the polymer matrix. An explanation of the conductivity enhancement phenomenon [2,3] which is now widely accepted for the solid samples is based on the assumption that the formation of amorphous domains on the matrix-filler interface occurs due to the polymer crystallization process inhibition on the grain surface. As the amorphous phase conductivity can be assumed on the basis of the NMR data to be about three orders of magnitude higher than the crystalline one, continuous percolation paths can be formed in the sample. A wide range of examples [3–6] can be found in literature to confirm the fact that the addition of nonconductive ceramic fillers such as alumina or silica to an electrolyte based on the PEO matrix leads to the conductivity improvement. A peak value in ambient temperature is near to 10^{-5} S cm^{-1} and can be obtained for composites containing 10–15% by weight of the dispersed particles. This value is about three orders of magnitude higher than for the pristine electrolyte and reaches the value characteristic for the amorphous phase of the PEO. For higher grain concentrations one can observe a decrease of conductivity as an effect of the synergetic combination of the polymer material dilution and amorphous phase stiffening. A semi-quantitative dependence of conductivity of the composite on the amount of the filler added can be divided into three separated regions. In the small filler concentration range only a very slight conductivity increase can be noticed. The obtained value is similar to the one characteristic for the basic electrolyte. A formation of the composite grains (consisting of a single grain and the generated shell) can be observed in the sample but the continuous percolation path is not yet achieved. A particular filler concentration can be found (dependent on the grain size, geometry and the shell thickness) for which the conductivity of the system increases abruptly. The observed maximum should achieve the values typical for the pure amorphous phase. For higher but still moderate amounts of the added grains a slow drop of the conductivity value should be observed due to the dilution effect. This situation is related to the fact that for the composition for which the maximum of conductivity is achieved all the polymeric material is already belonging to the grain shells. The excessive filler amount cannot, thus,

* Corresponding author. Tel.: +48 601 26 26 00; fax: +48 22 628 27 41.
E-mail address: alex@soliton.ch.pw.edu.pl (M. Siekierski).

0378-7753/$ – see front matter © 2007 Published by Elsevier B.V.
doi:10.1016/j.jpowsour.2007.05.063

lead to any further improvement of electrical parameters. An abrupt depletion is observed at the negative percolation point. This phenomenon can be attributed to the decay of continuity of the polymer matrix. The charge carrier transport is then blocked by the inert insulating filler grains. This phenomenon which is predicted by the model can be hardly observed for the experimental systems while the volume fraction of the filler needed is about 0.85.

1.1. Mesoscale models of conductivity

First mesoscale model applied for the calculations of conductivity in the composite polymeric electrolytes was the Effective Medium Theory [7,8]. It was based on the Maxwell–Garnett mixing rule for the calculations of effective conductivity of the composite unit (grain + shell) [9] and Landauer [10] and Bruggeman [11] works modified by Nan and Smith [12,13] and Nakamura [14] applied to the calculation of the final conductivity value of the composite for different percolation regimes. The main disadvantage of this successful approach is the need of an appropriate mixing rule for each studied geometry of the composite including such interesting phenomena as shell inhomogeneity, grain size and shape distribution. More versatile but on the other hand more complicated approaches to the simulation of the composites conductivity are based on the Finite Element [15,16] Finite Gradient [17,18] or Random Resistor Network (RRN). All three are based on the same concept of building of a virtual image of the simulated sample in the form of a two- or three-dimensional network of elements representing different fragments of the material studied. The main difference lies in the used algorithm of the network solving dependent on its varying creation rules.

RRN modeling is a widely recognized approach applied to different properties of heterogeneous materials consisting of regions of various properties. Apart from the electrical phenomena, magnetic properties of materials [19] or even the studies of sample destruction under critical mechanical stress [20] or geophysical studies of earthquakes [21] can be successfully performed by the means of this computational tool. When applied to electrical properties of the heterogeneous systems the method relates the value and type of a particular element to local properties of the sample. Resistivities, capacitances, parallel R-CPE connections can be used being adequate to conductors, insulators and other types of materials. Most of already published works (e.g. [22–24]) deal with very simple so-called binary systems being the image of the two-compound system. Usually, one of the components of the mixture is an insulator while the other one is a conductor. Electrical parameters of the branches (network elements) have only two valid values correlated to either a path (resistor) or an insulator (break). For such models an abrupt percolation threshold can be observed for a given composition of the sample represented by the particular number of either conducting (inserting conductors into insulating sample) or insulating (breaking the already conducting system) branches in the complete network.

Different more complicated systems were also studied by the means of the RRN approach [25–29]. Wang et al. [30] predict conductivity in composites consisting of the particles of metal and solid electrolyte. The simulated system consists of units of two different types to which either ionic or electronic conductivity can be attributed. To represent different types of materials present in the sample the authors use three resistive elements (metal–metal, metal–electrolyte and electrolyte–electrolyte connections) and two capacitors (geometrical capacity of the electrolyte and the double layer capacity of the electrolyte–metal junction). The phenomenon of double layer creation together with that of respective capacity presence is revealed at grain boundaries of different materials. An increase of average sample conductivity can be observed for compositions in which the percolation of metallic grains is observed.

A model of a system with similar geometry such as composite polymeric electrolytes with nonconductive filler is presented in [14]. Inorganic composites based on LiI/Al_2O_3 and $CuCl/Al_2O_3$ are studied. The authors assume that the highly conductive interfacial layer is built on the grain–matrix border. The main difference between the studied system and the polymeric systems lies in the fact that the insulating grains of the inorganic composite are not fully randomly located in the volume of the real sample. In the presented model randomly located (thus, the model is not in agreement with the real geometry) nodes (grains) are insulators. Sites not filled with the grain and, thus, belonging to the matrix exhibit ionic conductivity. The resistivity value for a branch is calculated on the basis of the status of its end nodes. If both belong to the grains the branch is broken (infinite resistivity) and if both belong to the matrix, the branch is the pristine conductor. In the case of a branch with ends placed in the nodes attributed to two different materials a high conductivity value is attributed. Finally, we must conclude that models presented in the literature from the point of view of the application in composite polymeric electrolytes are strongly oversimplified and, thus, cannot be applied without further elaboration. The main stress must be put on the finite thickness of the shell and its heterogeneity.

1.2. The proposed model

The proposed model is more sophisticated. It must be stressed that realization of so complicated calculations was possible only because of the increasing availability of high speed processors and large capacity memories in last few years. Finally, it is possible to deal with a 300^3 matrix filled with impedance data for the virtual sample represented as complex numbers. The initial part of the algorithm is related to the procedure of creation of a three-dimensional resistor network being a representation of morphology and phase structure of a sample of the simulated composition. At the beginning a virtual sample is built of the empty cubes. Then the location of spherical grains within the matrix is started. The procedure is based on random attributing a set of coordinates to the grain center. If a particular simulation assumes that grains are not identical a radius of a particular grain is also randomly chosen from a given range. Next, all cubic clusters belonging to the grain are marked using the following rule: the cluster belongs to the grain if the center of the cube lies inside it. This procedure is repeated until the assumed volume fraction

of the filler is achieved. As the ceramic material is not elastic and grains cannot overlay, each spatial unit can be attributed to only one grain. If a conflict of spatial restrictions is observed, during the next grain location an additional procedure changes the grain center coordinates and the check is performed once again. The algorithm also takes into consideration the insertion of grain fragments in the border area of the sample to observe the condition that analyzed fragment is a valid representation of a larger sample.

The residual part of the virtual sample (not belonging to grains) is then attributed to the shells (respecting the assumed shell thickness) and polymer electrolyte matrix (all cells belonging to neither the grain nor the shell). The values of characteristic impedances are attributed to all unitary cells on the basis of the assumed material parameters of all phases present in the system. The equivalent circuit used for the representation of each cell was a parallel combination of a resistor and a capacitor. At the end of this stage the virtual material is described as a three-dimensional network of impedances Z_{xyz}. Each cubic unit is electrically connected to its six neighbors (only the connections by the common walls are taken into consideration). The cell-oriented structure is then converted into a branch-oriented one with consequent location of the network nodes in the centers of the units. Each branch is, thus, characterized by an effective impedance value calculated as a serial connection of fractions originating from both neighboring cells.

A branch-oriented three-dimensional network obtained in this way can be solved in a various ways including both analytical and numerical approaches. For a matrix of the used size only numerical iteration procedures can be used. The applied algorithm uses a modification of the method introduced by Kirkpatrick [24] to find mean parameters of the heterogeneous network. To find the impedance of the sample the overall current must be calculated for a given test potential difference applied to the network. The current value is equal to the one found for any of the perpendicular layers of nodes in the sample. This value is found as a sum of currents in all branches located between nodes belonging to two neighboring layers. This observation is valid only in the stationary condition when the first Kirchoff's law is obeyed for each node (1).

$$\sum_i I_i = 0 \tag{1}$$

The network balancing is obtained by the attribution of proper potential values to all nodes in the network. Initial potentials values must be found as a starting point for the calculations. All the nodes located in the first and the last layer and, thus, attributed to the electrodes are fixed to potential values equal 0 and U respectively. The values of the intra-layer branch impedances in these layers are equal zero and the potentials are time-independent. Between them monotonic change of the potential is maintained by creating a set of equipotential layers of nodes. The value of the potential change between two neighboring layers is at this step constant. The initial potential distribution obtained in this way is later modified by the iteration procedure. In each of the iteration steps the value of each node potential is determined. A sum of currents for a node is calculated on the basis of the actual potential of the node, potentials of the neighboring nodes and the impedances of the braches located between them. Consequently, the potential of the node is changed in a manner allowing the fulfillment of the equation [1]. If it is not possible (as the value of the new node potential must lie in the range of the neighboring nodes voltages) the modified value is chosen to balance the node in the best possible manner. After performing the potential shifts for all nodes the whole procedure is repeated until the voltage distribution is stabilized. Consequently, the stationary state of the branch currents for all of the nodes should be reached in this way. The main disadvantage of the procedure described above lies in the fact that a quick stabilization of the local voltage distribution is reached, unfortunately, in the way which prevents global current stabilization. Therefore, an additional sub-procedure was created. It takes into consideration the interlayer currents forcing an additional modification of the node potentials in the beginning of the iteration process.

The total equalization of the currents in a 100^3 network is obtained in 10^4–10^5 iterations. This value is in the upper limit range taking into consideration the acceptable calculation time. Thus, for the used size of the matrix equal 300^3 there was a need of the change of the calculations termination criteria. The analysis of current changes for the following iteration steps in connection with an extrapolation procedure to obtain the final current value of the balanced network leads to at least one order of magnitude decrease in the needed calculation time allowing for the calculations of the large samples. We have proved by the test simulations that this modification does not affect the final conductivity value. In general the used model is a development of the dc model [31–33] previously described by us.

2. Experimental

OPEN MOSIX working on Slackware GNU/Linux was used to manage the computational cluster. C++ was used for code generation. The GNU C compiler was used to obtain the executables. The calculation times were in the range of a week for a set of data starting from 0 vol.% up to about 35 vol.% of the nonconductive additive. Electrical parameters for phases present in the system were given as follows: polymer matrix: $\sigma = 1 \times 10^{-8}$, $k = 4$; shell: $\sigma = 1 \times 10^{-4}$, $k = 8$; filler: $\sigma = 1 \times 10^{-12}$, $k = 10$. For some simulations (namely Fig. 4) modified values of the dielectric constants were applied to achieve a clarity of the phenomena described.

3. Results and discussion

The first interesting point of the study is the analysis of phase composition of the simulated electrolyte. A composite with grain diameter equal to 7 μm and shell thickness equal to 5 μm was chosen as a typical representative of the wide range of the materials of our interest. The concentrations of the particular phases present in the virtual sample are depicted in Fig. 1 as a function of the assumed amount of the added ceramic filler. Focusing on the shell amount one can observe a maximum located at about 15 vol.% of the filler. This observation is in good agreement with the maximum of the dc conductivity value (see Fig. 2). A second

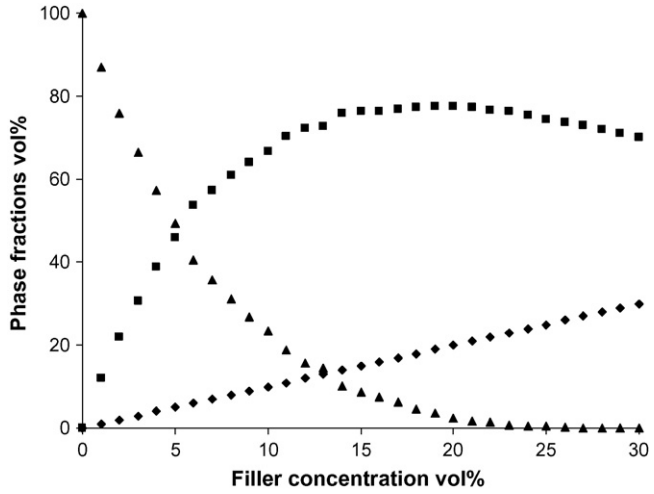

Fig. 1. Phase composition of the simulated samples as a function of the assumed filler concentration: (♦) grains, (■) grain shells, (▲) polymeric electrolyte matrix.

characteristic point is located at about 25 vol.% of the filler and can be described as an increase of the slope of the curve (quicker decrease of shell concentration starts here). When comparing with the curve related to the pristine polymeric matrix one can observe that this threshold is related to the total conversion of the matrix into shells (when the matrix concentration reaches zero). The conductivity plot also changes here its slope to more negative. This set of dependencies together with both linear decrease of conductivity and shell volume fraction above this point shows clearly that in this filler concentration range (25–30 vol.%) the model predicts conductivity changes related to the dilution of already fully converted polymeric material by the excess of the filler.

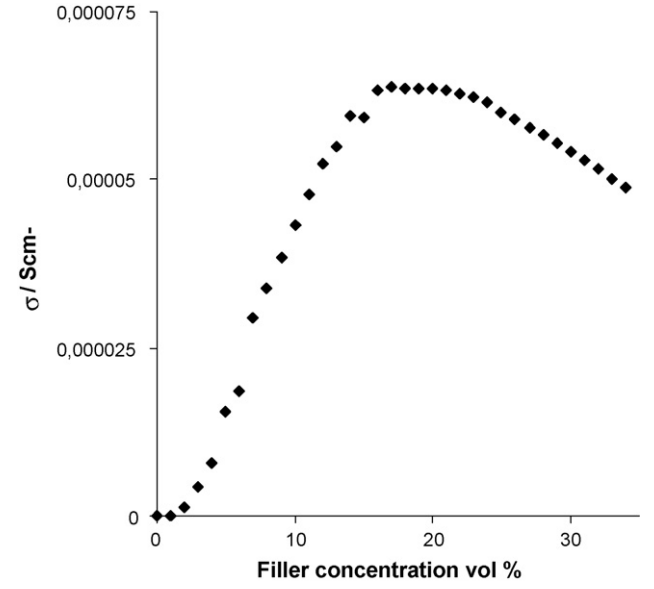

Fig. 2. Simulated dc conductivity of the set of samples as a function of the filler amount. Values of conductivity calculated from the ac model for frequency equal 0.

The comparison of the shell phase amount and virtual sample conductivity as a function of the filler contents for samples characterized by various grain diameter and constant shell thickness is shown in the Fig. 3a and b, respectively. One can easily observe that the shape of the curve describing the phase composition (a) is strongly dependent on the assumed grain diameter. An increase of this parameter leads, firstly, to a shift of the maximum location to higher filler amounts. Secondly, the maximal value is lower for higher grain diameters. Additionally, the slope of the increasing branch of the curve is lower and the maximum is more flat. For very high grain concentrations all curves overlap (about 30 vol.%) showing that above that point only a dilution of the shells originating from the already converted polymer matrix by

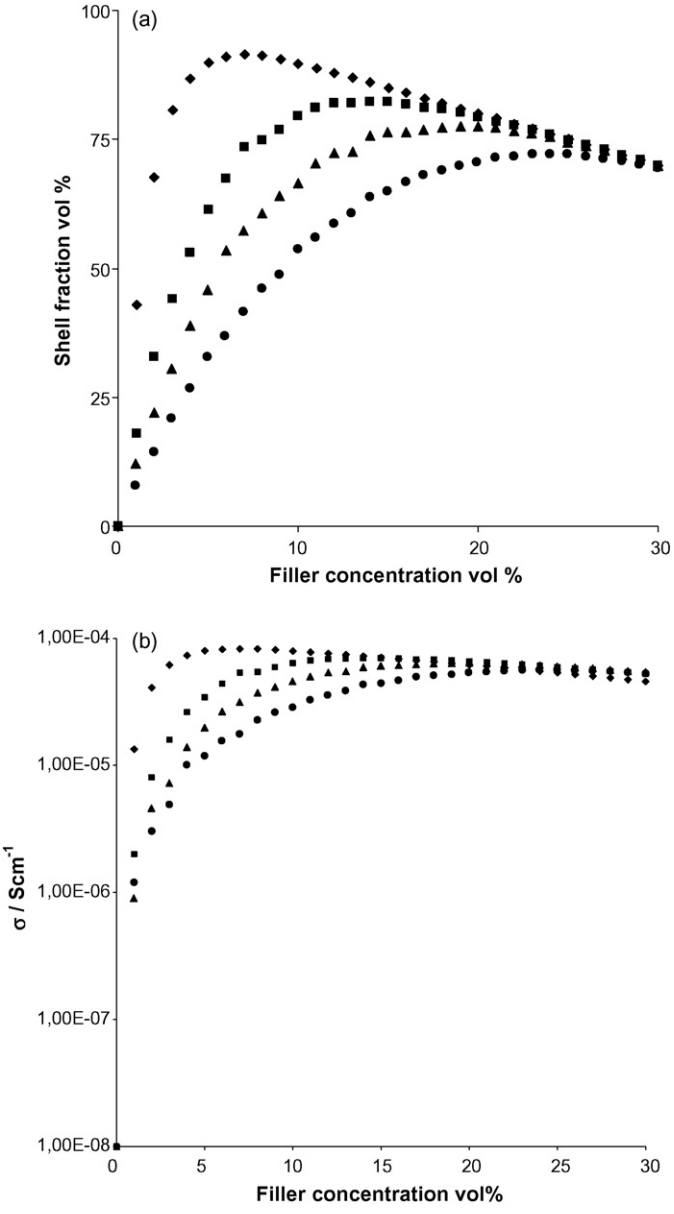

Fig. 3. (a) A set of the shell volume fraction dependencies on the filler amount for samples with various grain diameter and constant shell thickness (5 μm), (b) a set of the conductivity dependencies on the filler amount for the same samples: (♦) $d = 3$ μm, (■) $d = 5$ μm, (▲) $d = 7$ μm, (●) $d = 9$ μm.

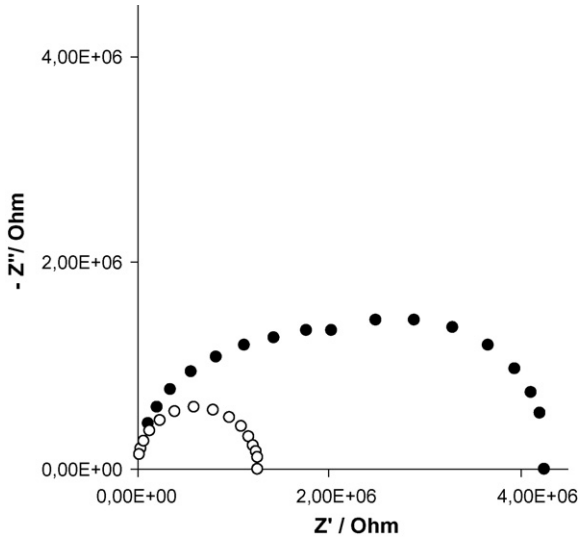

Fig. 4. A comparison of the simulated high frequency dielectric response of the 10 vol% composite sample: (●) grain diameter $d = 5\,\mu m$, shell thickness $t = 3\,\mu m$, (◯) grain diameter $d = 5\,\mu m$, shell thickness $t = 7\,\mu m$.

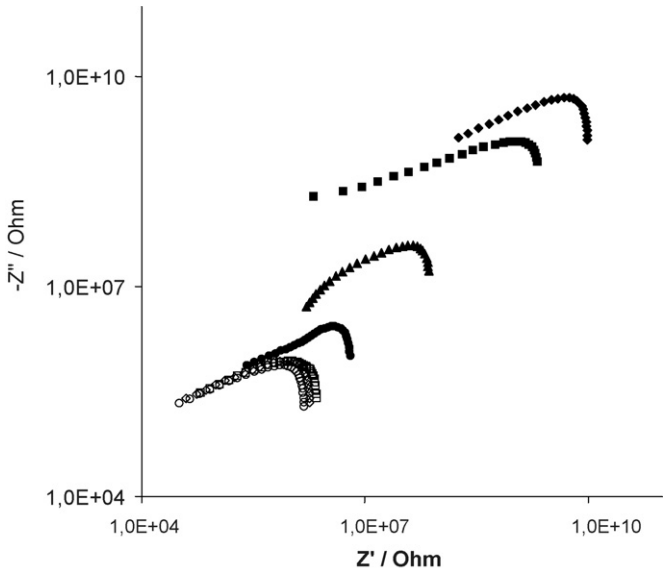

Fig. 5. A set of high frequency simulated impedance spectra calculated for a virtual sample characterized by $d = 7\,\mu m$ and $t = 5\,\mu m$. Filler fraction equal to: (♦) 0 vol.%, (■) 1 vol.%, (▲) 2 vol.%, (●) 5 vol.%, (□) 10 vol.%, (◯) 20, (◊) 30 vol.%.

the excessive filler grains can be observed. Similar dependencies can be observed on the conductivity curve (Fig. 3b) showing that, in general, the conductivity value changes follow the changes in the amount of the shell phase.

Fig. 4 shows the simulated high frequency dielectric response for two virtual samples of the composite electrolyte containing 10 vol.% of the filler characterized by the grain diameter equal to 5 μm. The difference lies in the applied thickness of the amorphous shell formed on the grain surface. In the first case (filled dots) it is equal to 3 μm in the latter (empty dots) to 7 μm. One can easily observe that the change of thickness leading, in consequence, to the change of the network units allocated to shells results not only in the change of the impedance value (a decrease of about four times for the more modified sample) but also to the change of the conductivity mechanism. In the first case the amorphous shells do not form the continuous percolation paths yet. A conductivity value is intermediate between the pristine electrolyte and the maximum possible. Both materials (pristine polymer and amorphous shells) are characterized by different impedance properties leading to a different time constant of the respective Nyquist semi-circle ($\tau = RC$). Two merged semi-circles observed can be attributed to the parts of current flowing through shell phase and the pristine polymer. In the case of the assumed stronger interaction of the filler with the polymer 10 vol.% composition is characterized with almost full conversion of the polymeric material. Thus, the only single time constant can be observed in the spectra giving as a result only one semicircle.

To compare the calculated ac high frequency dielectric response of composite virtual samples containing various amount of the filler (and constant filler diameter equal to $d = 7\,\mu m$ and shell thickness equal to $t = 5\,\mu m$) one must apply a modified Nyquist representation. Because of the very broad range of the impedance value changes a logarithmic scale was used to present the data for the unmodified sample and for the composite electrolytes on one plot (Fig. 5). It can be observed that most significant difference in the values of the impedance can be found for virtual samples with the filler amount between 0 and 10 vol.%. Later, the changes of both imaginary and real part of the impedance are smaller. A monotonically decreasing tendency is observed between 0 and 20 vol.% of the filler. For 30 vol.% sample a slight increase of the impedance is observed as the sample is located on the negatively sloped branch of the curve depicting the conductivity-composition dependence. Additionally, one can observe that the shape of the curves is identical for the pristine and highly modified electrolyte. In contrast, the curves located near the abrupt conductivity change composition (2 and 5 vol.%) exhibit a slightly different shape. This phenomenon can be also attributed to the mechanism of conductivity based on simulataneous charge transportation in the electrolyte bulk and in highly conductive shells for these samples.

A more detailed difference can be observed using the linear (classical) Nyquist plot. In this case data for both pristine and modified systems cannot be clearly depicted on one graph. Thus, a comparison of moderately and highly doped samples is presented in Fig. 6. The set of impedance spectra was calculated for samples of various filler concentration and for grain diameter $d = 3\,\mu m$ and shell thickness $t = 5\,\mu m$. The assumed values allow us to observe the changes of the curve shape for relatively low filler concentrations as the increase of the shell phase amount is quick (compare with Fig. 3a). Here one can perfectly see that while most of the tested compositions lead to one semicircle image the lowest one (1%) gives a strongly deformed spectrum in which the contribution of the matrix and shells can be found. In this sample the total conductivity is also a combination of bulk and shell charge transport, both characterized by different types of material involved (semi-crystalline matrix and amorphous shell). Two partially separated time constants can be, thus, attributed to the mechanism of conductivity based on simultaneous charge transportation in the electrolyte bulk and

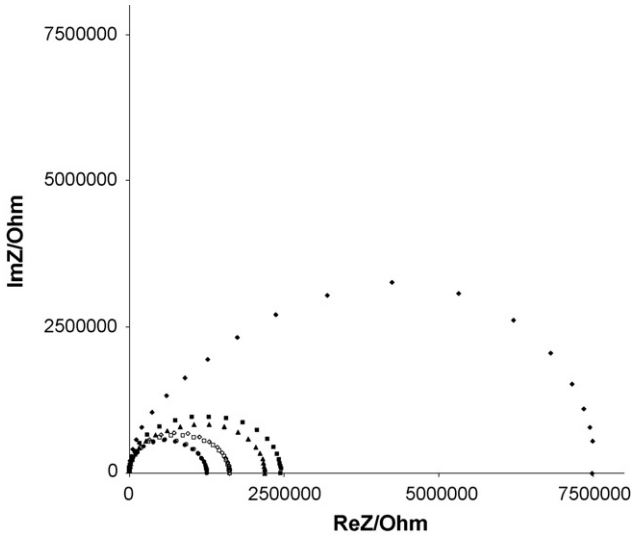

Fig. 6. A set of high frequency simulated impedance spectra calculated for a virtual sample characterized by $d = 3$ μm and $t = 5$ μm. Filler fraction equal to: (♦) 1, (■) 2, (◊) 3, (○) 5, (●) 10, (□) 20, (▲) 30 vol.%.

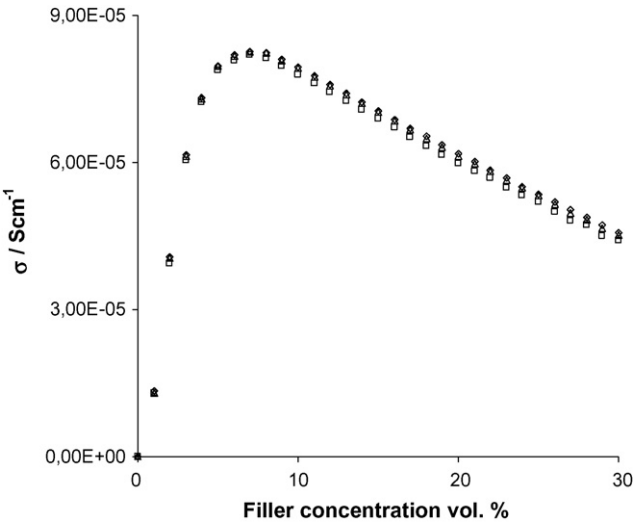

Fig. 7. Simulated dc conductivity values found from the ac spectra of the virtual sample as a function of filler concentration. Calculations performed in various manners: (◊) extrapolation of the Z' to $\omega = 0$, (□) diameter of the semi-circle, (△) zero point of the semi-circle.

in highly conductive shell. Also an interesting phenomenon can be observed for 2 and 30 vol.% samples which both give the almost identical impedance spectra in the form of a depressed semi-circle. This observation is also valid for the 3 and 20 vol.% pair and for the 5 and 10 vol.% pair of samples. In the later case, the obtained semi-circles are only slightly deformed as the sample compositions are located around the conductivity maximum. The case of the 3 and 20 vol.% pair is between of the middle of the two terminal pairs. Finally, it must be stressed that for moderate and strongly modified samples only one time constant can be observed because only one charge transport mechanism related to the amorphous shells is present in the sample. The similarity of the pairs of images found below and above the maximum of the conductivity is related to the oversimplification of the model based on the assumption of the shell homogeneity. As was previously proved, for dc calculations [33] this approach produces a partially false image of the samples containing large amounts of the dispersed filler.

Finally, the problem of the method used for the calculation of the dc conductivity value from the ac impedance spectra can be analyzed. A reference method is the extrapolation of the Z' values to the frequency equal zero. This method gives values identical with the ones given by the direct application of the previously tested dc RRN approach [31–33]. For comparison, the values calculated from the diameter of the ac semi-circle and from its zero point were plotted together (Fig. 7). For both semi-circle based methods the values were calculated not taking into consideration the spectrum depression and time constants separation (treating data as a one semi-circle). One can see that the shapes of the obtained curves are identical and the obtained values are very similar. A relative error plot was depicted in Fig. 8. One can see that both methods work in the whole range of filler amount with the relative error value lower than 5%. The method based on the zero point is much more adequate producing a few times lower relative error values. Both curves have similar shapes with the minimum located near the maximum of conductivity. This observation can be related to the fact that for these samples the obtained spectra are much closer to the ones predicted for the parallel RCPE connection. The discrepancy of the error values is more pronounced for the high filler amount where the obtained spectra form a depressed semi-circle showing that in this case the zero-point method produces results closer to the expected ones. A smaller difference observed for the slightly modified samples shows that both methods are not ideal for a merged two semi-circle spectrum characteristic for the regime in which mechanism of conductivity is based on simultaneous charge transportation in the electrolyte bulk and in highly conductive shells.

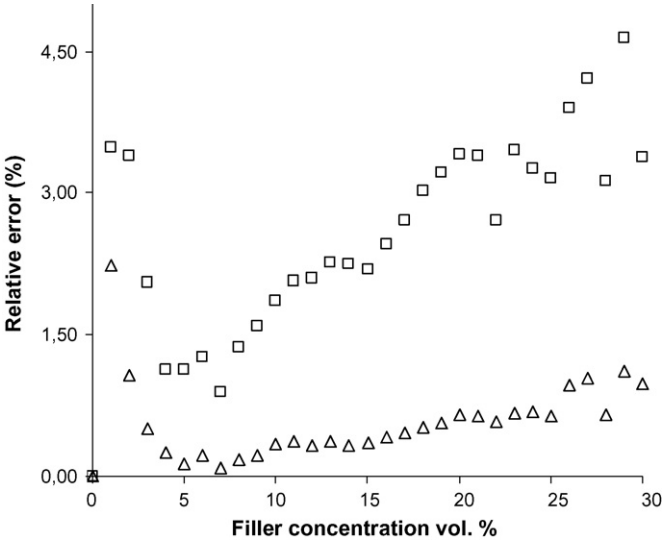

Fig. 8. Relative errors of the simulated dc conductivity values found from the ac spectra of the virtual sample as a function of filler concentration. Calculations performed in various manners (extrapolation of the Z' to $\omega = 0$ as a reference): (□) diameter of the semi-circle, (△) zero point of the semi-circle.

4. Conclusions

The Random Resistor Network approach was successfully applied to the simulation of ac electrical properties of composite polymeric electrolytes. The obtained data are in good agreement with the previously published data coming both from impedance spectroscopy measurements and the Effective Medium Theory simulations. The observed changes of the computed conductivity value follow, in general, the observed phase structure modification leading to an increase of the highly conductive phase content. For a small amount of grains added one can observe an increase of the conductivity value which is also present for the virtual systems studied. The slope of the curve and the position of the maximum vary with the changes of grain size and the shell thickness. The behavior observed can be attributed to the increase of the highly conductive shell contents. Additionally, a second time constant can be found in some impedance spectra of the slightly modified samples for filler amount values around the abrupt conductivity change composition. The conductivity maximum can be attributed to the total conversion of the sample volume (disregarding the units belonging to the grains) into highly conductive amorphous shells. No more spatial units can be attributed to the pristine polymeric matrix. In the ac image this range can be described as the well defined single semi-arc type spectrum. The following conductivity drop is related to a decrease in the number of clusters containing the polymeric material due to the dilution effect of the excessive filler grains. In the ac spectra this phenomenon can be attributed to the depression of the previously observed single semi-arc.

The proposed model is very versatile and can be easily modified to cover systems more complicated and, thus, closer to reality. The main possible modification (already realized for the dc approach) is related to the introduction of the defined conductivity distribution within the highly conductive amorphous shell. This operation should allow taking into the consideration the stiffening phenomenon observed for composites containing ceramic fillers. The exchange of nonconductive grains for conductive ones is also possible and allows a study of so-called mixed-phase composites together with their grain boundary properties.

Acknowledgments

The authors of this paper would like to acknowledge the help of all their co-workers from the Warsaw University of Technology. Special thanks are given to Prof. Władysław Wieczorek, Prof. Franciszek Krok, Dr. Józef Dygas and Mr. Henryk Wyciślik for valuable comments and discussions. Mr. Andrzej Łukaszewicz is kindly acknowledged for the proofreading of the manuscript. Mr. Marcin Bukat is kindly acknowledged for the GNU/Linux–Open MOSIX cluster maintenance. GNU/Linux international community is acknowledged for the open source software development allowing cost reduction of the simulations. Warsaw University of Technology is kindly acknowledged for the financial support of the presented work.

References

[1] A.S. Aricò, P. Bruce, B. Scrosati, J.-M. Tarascon, W. van Schalkwijk, Nat. Mater. 4 (2005) 366–377.
[2] J. Weston, B.C.H. Steele, Solid State Ionics 7 (1982) 75.
[3] W. Wieczorek, K. Such, H. Wyciślik, J. Płocharski, Solid State Ionics 36 (1989) 255.
[4] J. Przyłuski, Z. Florjańczyk, K. Such, H. Wyciślik, W. Wieczorek, Synth. Met. 35 (1989) 241.
[5] S. Skaarup, K. West, B. Zachau-Christiansen, Solid State Ionics 28-30 (1988) 979.
[6] J. Zhou, P.S. Fedkiw, Solid State Ionics 3–4 (2004) 275.
[7] W. Wieczorek, M. Siekierski, J. Appl. Phys. 76 (1994) 2220.
[8] M. Siekierski, J. Przyłuski, W. Wieczorek, Electrochim. Acta 40 (11–14) (1995) 2101.
[9] J.C. Maxwell, A Treaty on Electricity and Magnetism, vol. 1, Clerendon, London, 1892 (Chapter XI).
[10] R. Landauer, J. Appl. Phys. 23 (1952) 779.
[11] D.A.G. Bruggeman, Ann. Phys. (Leipzig) 24 (1935) 636.
[12] C.W. Nan, Progr. Mater. Sci. 37 (1993) 1.
[13] C.W. Nan, D.M. Smith, Mater. Sci. Eng. B10 (1991) 99.
[14] M. Nakamura, Phys. Rev. B29 (1984) 3691.
[15] J. Fleig, J. Maier, J. Electrochem. Soc. 145 (1998) 2081.
[16] J. Fleig, J. Maier, Electrochim. Acta 41 (1996) 1003.
[17] R.T. Coverdale, H.M. Jennings, E.J. Garboczi, Comp. Mater. Sci. 3 (1995) 465.
[18] R.T. Coverdale, E.J. Garboczi, B.J. Christensen, T.O. Manson, H.M. Jennings, J. Am. Ceram. Soc. 76 (1993) 1153.
[19] Xu, P.M. Hui, Z.Y. Li, J. Appl. Phys. 90 (2001) 365.
[20] M. Acharyya, B.K. Chakrabarti, J. Phys. (Paris) I5 (1995) 153.
[21] M. Acharyya, B.K. Chakrabarti, Phys. A 224 (1996) 254.
[22] S. Jiang, J.B. Wagner Jr., J. Phys. Chem. Solids 56 (1995) 1113.
[23] E.C. Yeh, M. Chiou, K.Y. Hsu, Thin Solid Films 297 (1997) 88.
[24] S. Kirkpatrick, Rev. Mod. Phys. 45 (1973) 574.
[25] J. Bigalke, Phys. A 272 (1999) 281.
[26] D.G. Han, G.M. Choi, Solid State Ionics 106 (1998) 71.
[27] J.J.S. Andrade, Y. Shibusa, Y. Arai, A. Siqueira, Synth. Met. 68 (1995) 167.
[28] C. Pennetta, L. Reggiani, E. Alfinito, G. Trefan, J. Phys. Condens. Matter 14 (2002) 2371.
[29] O. Stenull, H.K. Janssen, Phys. Rev. E 6405 (2001) 65105.
[30] J. Wang, Y. Wang, Z. Li, Phys. Lett. A 244 (1998) 30.
[31] M. Siekierski, P. Rzeszotarski, K. Nadara, Solid State Ionics 176 (2005) 2129.
[32] K. Nadara, M. Siekierski, Solid State Ionics 176 (2005) 1781.
[33] M. Siekierski, K. Nadara, Electrochim. Acta 50 (2005) 3796.